Structure of the Modified Heme in Allylbenzene-Inactivated Chloroperoxidase Determined by Q-Band CW and Pulsed ENDOR

Hong-In Lee,[†] Annette F. Dexter,[‡] Yang-Cheng Fann,[†] Frederick J. Lakner,[‡] Lowell P. Hager,[‡] and Brian M. Hoffman*,[†]

Contribution from the Department of Chemistry, Northwestern University, Evanston, Illinois 60208-3113, and Department of Biochemistry, University of Illinois, Urbana, Illinois 61801

Received October 23, 1996[⊗]

Abstract: During the epoxidation of allylbenzene, chloroperoxidase (CPO) is converted to an inactive green species in which the prosthetic heme has been modified by addition of the alkene plus an oxygen atom (Dexter, A. F.; Hager, L. P. *J. Am. Chem. Soc.* **1995**, *117*, 817−818). We have used Q-band continuous wave and pulsed electron-nuclear double resonance (ENDOR) spectroscopy to study the CPO heme *in situ* following inactivation with allylbenzene, using samples prepared in natural isotopic abundance, with ^{15}N-labeled enzyme, and with allylbenzene labeled with ^{2}H or ^{13}C in specific vinylic positions. The electron paramagnetic resonance (EPR) spectrum of the inactivated enzyme is dominated by a low-spin ferric signal ($g_{1,2,3} = 2.32, 2.16, 1.95$). ^{14,15}N ENDOR examination of allylbenzene-inactivated CPO reveals that three nitrogens of the heme are similar, but the fourth nitrogen is markedly different, suggesting that a single pyrrole ring has been covalently modified at the unique nitrogen. These studies also reveal the orientation of the **g** tensor relative to the heme. ^{13}C ENDOR of allylbenzene-inactivated CPO with ^{13}C-labeled allylbenzene shows that the C-1 and C-2 carbons of allylbenzene are covalently connected to the heme system. ^{1,2}H ENDOR plus mass analysis of CPO heme after inactivation with deuterated allylbenzene show that all three vinylic protons are retained in the heme adduct. No strongly-coupled exchangeable protons are observed, indicating that the axially bound water of frozen native CPO has been displaced. The ^{1}H at the C-2 position of the alkene shows strong, mostly isotropic hyperfine coupling while the two hydrogens at the C-1 position show weak, dipolar couplings. The hyperfine tensors of ^{1,2}H of the C-1 position of allylbenzene have been determined, and give the position of these atoms relative to the heme. These data, combined with molecular modeling calculations, have been used to deduce that the allylbenzene-bound heme of inactivated CPO is an *N*-alkylhemin metallocycle with C-1 of allylbenzene bonded to the pyrrole nitrogen and to obtain metrical details of its structure.

Chloroperoxidase (CPO)[1] is a highly versatile heme enzyme that catalyzes the oxidation of a broad range of substrates with hydrogen peroxide as oxidant. During the catalytic cycle, native ferric CPO reacts with hydrogen peroxide to form a two-electron oxidized intermediate, compound **I**, which then reacts with an organic or inorganic substrate to regenerate the ferric enzyme and an oxidized species (Scheme 1). The first reaction reported to be catalyzed by CPO was the halogenation of organic substrates.[2] Recent interest in CPO has focused on its capacity for the epoxidation of alkenes.[3] While the ability to epoxidize alkenes in an oxo-transfer reaction is common to a number of enzymatic and model heme systems, CPO is of interest in that it catalyzes the oxo-transfer with high facioselectivity, leading to enantiomerically enriched products.

Scheme 1

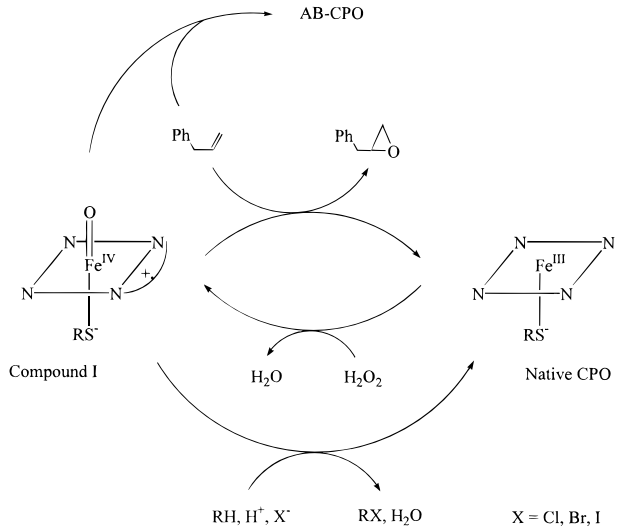

In a number of heme enzyme and heme model systems, the catalytic epoxidation of monosubstituted alkenes is accompanied by an autoinactivation reaction that produces modified hemins containing the alkene skeleton. The formation of these "green pigments" was first observed with hepatic microsomal cytochrome P450 (P450) *in vivo*,[4] and has since been demonstrated with several model hemins[5,6] and more recently in our laboratory with chloroperoxidase (CPO).[3a,7] Surprisingly, the heme−alkene adducts spontaneously revert to the native heme on

[†] Northwestern University.

[‡] University of Illinois.

[⊗] Abstract published in *Advance ACS Abstracts,* April 15, 1997.

(1) Abbreviations used: AB-CPO (allylbenzene−CPO), green enzyme species produced by reaction of native CPO with allylbenzene and hydrogen peroxide; CPO, chloroperoxidase; CW, continuous wave; DEAE, (diethylamino)ethyl; EDTA, ethylenediaminetetraacetic acid; ENDOR, electron nuclear double resonance spectroscopy; EPR, electron paramagnetic resonance spectroscopy; hemin, iron(III) porphyrin; MS, mass spectroscopy; NMR, nuclear magnetic resonance spectroscopy; P450, cytochrome P450; RF, radio frequency; R_z, purity number A_{400}/A_{280}; THF, tetrahydrofuran.

(2) Shaw, P. D.; Hager, L. P. *J. Biol. Chem.* **1960**, *236*, 1626−1630.

(3) (a) Dexter, A. F.; Lakner, F. J.; Campbell, R. A.; Hager, L. P. *J. Am. Chem. Soc.* **1995**, *117*, 6412−6413. (b) Colonna, S.; Gaggero, N.; Casella, L.; Carrea, G.; Pasta, P. *Teteahedron: Asymmetry* **1993**, *4*, 1325−1330. (c) Lakner, F. J.; Hager, L. P. *J. Org. Chem.* **1996**, *61*, 3923−3925. (d) Allain, E. J.; Hager, L. P.; Deng, L.; Jacobsen, E. N. *J. Am. Chem. Soc.* **1993**, *115*, 4415−4416.

S0002-7863(96)03684-0 CCC: $14.00

standing, with both CPO[7] and model systems.[6] A similar reversibility for the P450 inactivation reaction has been predicted,[6c] but has not been reported.

In all alkene-modified heme systems studied to date, *N*-(2-hydroxyalkyl)porphyrins (**1**) containing the alkene skeleton (or their oxidized derivatives)[5c,e] can be isolated from the epoxidation reaction following acid demetalation of the hemin. At least five distinct heme adducts might give rise to this chemistry: three metallocycles (**2**−**4**) with differing Fe,N bridge lengths;[6,8] a β-hydroxycarbene (**5**);[9] and a σ-alkylhemin (**6**).[10]

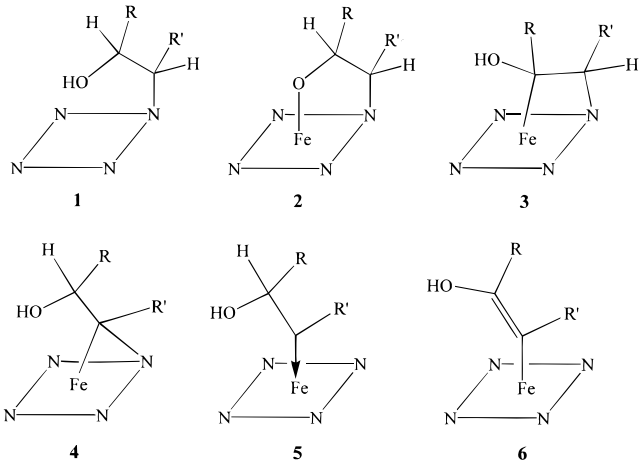

In each case, two orientations of addition are possible for a monosubstituted alkene (R or R′ = H), for a total of ten different possible structures. The *N*-(2-hydroxyalkyl)porphyrins isolated from alkene-inactivated enzymatic or model systems after acid treatment are simple demetalation products of **2**. However, the same demetalated porphyrins might also arise by rearrangement of the organometallic species **3**−**6** under the conditions of workup.[11] It is known from a variety of model[8,10−12] and enzymatic[13] heme systems that organometallic heme species including porphyrin iron carbenes and σ-alkyliron porphyrins (and their σ-aryl or σ-vinyl analogs) (i) may be generated under catalytic conditions and (ii) undergo a reversible, redox-induced metal-to-nitrogen ligand migration to yield N-substituted porphyrin products. Ligand migration of this kind has been proposed to be responsible for the isolation of N-substituted porphyrins from heme enzyme systems following inactivation with xenobiotics including alkyl (or aryl) hydrazines,[13] sydnones,[14] collidine derivatives,[15] and griseofulvin.[16]

On the basis of results with model hemins, the recent consensus is that the products of alkene-mediated inactivation in both model and enzymatic systems are *N*-alkylhemin metallocycles of type **2**.[4−6] For the model systems, this structural assignment appears well founded. NMR studies of an intact alkene-modified tetraarylhemin[6b] have shown shifts in one set of β-pyrrole proton resonances, consistent with covalent modification of a single pyrrole ring and with ^{1}H shifts seen in synthetic *N*-alkylhemins.[17] While an observed shift in NMR resonances for one set of pyrrole protons does not discriminate between structures **2**−**4**, reconstitution of *N*-(2-hydroxyalkyl)-porphyrins with Fe(III) and appropriate ligands gives hemins with electronic spectra similar to those of the primary products of alkene-mediated inactivation,[6a,b] and the EPR and optical spectra of these hemins are consistent with axial alkoxide ligation, as opposed to σ-alkyl ligation.

To date, no comparable structural studies have been carried out on the intact enzymatic heme adducts. For P450, *in situ* studies of the modified hemin have been hampered by the difficulty of obtaining sufficiently clean preparations of inactivated enzyme, although detailed NMR studies have been conducted on demetalated porphyrins isolated from P450. *N*-(2-Hydroxyalkyl)protoporphyrin IX derivatives isolated from alkene-inactivated P450 reveal a marked regioselectivity and stereoselectivity of pyrrole N-alkylation, suggesting that the pyrrole alkylation occurs within the enzyme active site.[4a,b] However, enzyme reconstitution with an alkene-modified hemin

(4) (a) Kunze, K. L.; Mangold, B. L. K.; Wheeler, C.; Beilan, H. S.; Ortiz de Montellano, P. R. *J. Biol. Chem.* **1983**, *258*, 4202−4207. (b) Ortiz de Montellano, P. R.; Mangold, B. L. K.; Wheeler, C.; Kunze, K. L.; Reich, N. O. *J. Biol. Chem.* **1983**, *258*, 4208−4213. (c) Ortiz de Montellano, P. R.; Correia, M. A. In *Cytochrome P450: Structure, Mechanism, and Biochemistry*, 2nd ed.; Ortiz de Montellano, P. R., Ed.; Plenum Press: New York, 1995; pp 305−364. (d) Shirane, N.; Sui, Z.; Peterson, J. A.; Ortiz de Montellano, P. R. *Biochemistry* **1993**, *32*, 13732−13741.

(5) (a) Mansuy, D.; Devocelle, L.; Artaud, I.; Battioni, J.-P. *Nouv. J. Chem.* **1985**, *9*, 711−716. (b) Collman, J. P.; Hampton, P. D.; Brauman, J. I. *J. Am. Chem. Soc.* **1986**, *108*, 7861−7862. (c) Artaud, I.; Devocelle, L.; Battioni, J.-P.; Girault, J.-P.; Mansuy, D. *J. Am. Chem. Soc.* **1987**, *109*, 3782−3783. (d) Artaud, I.; Grégoire, N.; Mansuy, D. *New J. Chem.* **1989**, *13*, 581−586. (e) Nakano, T.; Traylor, T. G.; Dolphin, D. *Can. J. Chem.* **1990**, *68*, 1504−1506. (f) Collman, J. P.; Hampton, P. D.; Brauman, J. I. *J. Am. Chem. Soc.* **1990**, *112*, 2977−2986. (g) Collman, J. P.; Hampton, P. D.; Brauman, J. I. *J. Am. Chem. Soc.* **1990**, *112*, 2986−2998.

(6) (a) Mashiko, T.; Dolphin, D.; Nakano, T.; Traylor, T. G. *J. Am. Chem. Soc.* **1985**, *107*, 3735−3736. (b) Traylor, T. G.; Nakano, T.; Miksztal, A. R.; Dunlap, B. E. *J. Am. Chem. Soc.* **1987**, *109*, 3625−3632. (c) Tian, Z.-Q.; Richards, J. L.; Traylor, T. G. *J. Am. Chem. Soc.* **1995**, *117*, 21−29.

(7) Dexter, A. F.; Hager, L. P. *J. Am. Chem. Soc.* **1995**, *117*, 817−818.

(8) (a) Chevrier, B.; Weiss, R.; Lange, M.; Chottard, J.-C.; Mansuy, D. *J. Am. Chem. Soc.* **1981**, *103*, 2899−2901. (b) Latos-Grazynski, L.; Cheng, R.-J.; La Mar, G. N.; Balch, A. L. *J. Am. Chem. Soc.* **1981**, *103*, 4270−4272. (c) Mansuy, D.; Morgenstern-Badarau, I.; Lange, M.; Gans, P. *Inorg. Chem.* **1982**, *21*, 1427−1430. (d) Olmstead, M. M.; Cheng, R.-J.; Balch, A. L. *Inorg. Chem.* **1982**, *21*, 4143−4148. (e) Balch, A. L.; Cheng, R.-J.; La Mar, G. N.; Latos-Grazynski, L. *Inorg. Chem.* **1985**, *24*, 2651−2656.

(9) (a) Groves, J. T.; Avaria-Neisser, G. D.; Fish, K. M.; Imachi, M.; Kuczkowski, R. L. *J. Am. Chem. Soc.* **1986**, *108*, 3837−3838. (b) Dolphin, D.; Matsumoto, A.; Shortman, C. *J. Am. Chem. Soc.* **1989**, *111*, 411−413.

(10) (a) Lexa, D.; Savéant, J.-M.; Battioni, J.-P.; Lange, M.; Mansuy, D. *Angew. Chem., Int. Ed. Engl.* **1981**, *20*, 578−579. (b) Battioni, P.; Mahy, J. P.; Gillet, G.; Mansuy, D. *J. Am. Chem. Soc.* **1983**, *105*, 1399−1401. (c) Tabard, A.; Cociolos, P.; Lagrange, G.; Gerardin, R.; Hubsch, J.; Lecomte, C.; Zarembowitch, J.; Guilard, R. *Inorg. Chem.* **1988**, *27*, 110−117. (d) Guilard, R.; Kadish, K. M. *Chem. Rev.* **1988**, *88*, 1121−1146.

(11) (a) Lange, M.; Mansuy, D. *Tetrahedron Lett.* **1981**, *22*, 2561−2564. (b) Ortiz de Montellano, P. R.; Kunze, K. L.; Augusto, O. *J. Am. Chem. Soc.* **1982**, *104*, 3545−3546. (c) Lançon, D.; Cociolos, P.; Guilard, R.; Kadish, K. M. *J. Am. Chem. Soc.* **1984**, *106*, 4472−4478. (d) Balch, A. L.; Renner, M. W. *J. Am. Chem. Soc.* **1986**, *108*, 2603−2608. (e) Mansuy, D.; Battioni, P.; Battioni, J.-P. *Eur. J. Biochem.* **1989**, *184*, 267−285.

(12) (a) Callot, H. J.; Schaeffer, E. *Tetrahedron Lett.* **1980**, *21*, 1335−1338. (b) Mansuy, D.; Battioni, J.-P.; Dupré, D.; Sartori, E.; Chottard, G. *J. Am. Chem. Soc.* **1982**, *104*, 6159−6161. (c) Mansuy, D. *Pure Appl. Chem.* **1987**, *59*, 759−770. (d) Artaud, I.; Gregoire, N.; Battioni, J.-P.; Dupre, D.; Mansuy, D. *J. Am. Chem. Soc.* **1988**, *110*, 8714−8716.

(13) (a) Jonen, H. G.; Werringloer, J.; Prough, R. S.; Estabrook, R. W. *J. Biol. Chem.* **1982**, *257*, 4404−4421. (b) Battioni, P.; Mahy, J.-P.; Delaforge, M.; Mansuy, D. *Eur. J. Biochem.* **1983**, *134*, 241−248. (c) Ringe, D.; Petsko, G. A.; Kerr, D. E.; Ortiz de Montellano, P. R. *Biochemistry* **1984**, *23*, 2−4. (d) Raag, R.; Swanson, B. A.; Poulos, T. L.; Ortiz de Montellano, P. R. *Biochemistry* **1990**, *29*, 8119−8126. (e) Samokyszyn, V. M.; Ortiz de Montellano, P. R. *Biochemistry* **1991**, *30*, 11646−11653. (f) Mahy, J. P.; Gaspard, S.; Mansuy, D. *Biochemistry* **1993**, *32*, 4014−4021. (g) Gerber, N. C.; Ortiz de Montellano, P. R. *J. Biol. Chem.* **1995**, *270*, 17791−17796.

(14) (a) Grab, L. A.; Swanson, B. A.; Ortiz de Montellano, P. R. *Biochemistry* **1988**, *27*, 4805−4814. (b) Ortiz de Montellano, P. R.; Grab, L. A. *J. Am. Chem. Soc.* **1986**, *108*, 5584−5589.

(15) (a) Ortiz de Montellano, P. R.; Beilan, H. S.; Kunze, K. L. *J. Biol. Chem.* **1981**, *256*, 6708−6713. (b) Ortiz de Montellano, P. R.; Beilan, H. S.; Kunze, K. L. *Proc. Natl. Acad. Sci. U.S.A.* **1981**, *78*, 1490−1494.

(16) (a) De Matteis, F.; Gibbs, A. H.; Martini, S. R.; Milek, R. L. B. *Biochem. J.* **1991**, *280*, 813−816. (b) Holley, A. E.; Frater, Y.; Gibbs, A. H.; De Matteis, F.; Lamb, J. H.; Farmer, P. B.; Naylor, S. *Biochem. J.* **1991**, *274*, 843−848.

(17) (a) Balch, A. L.; Chan, Y.-W.; La Mar, G. N.; Latos-Grazynski, L.; Renner, M. W. *Inorg. Chem.* **1985**, *24*, 1437−1443. (b) Balch, A. L.; La Mar, G. N.; Latos-Grazynski, L.; Renner, M. W. *Inorg. Chem.* **1985**, *24*, 2432−2436. (c) Balch, A. L.; Cornman, C. R.; Latos-Grazynski, L.; Olmstead, M. M. *J. Am. Chem. Soc.* **1990**, *112*, 7552−7558.

has not been realized for either P450 or CPO. At the same time, very few spectroscopic studies have been carried out on the intact alkene-inactivated enzymes, hindering comparisons with model hemins.

During the epoxidation of allylbenzene (**7**), chloroperoxidase

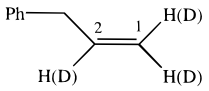

7

(CPO) is converted to an inactive green species in which the prosthetic heme has been modified by addition of the alkene plus an oxygen atom.[7] In the present work we have used Q-band continuous wave (CW) and pulsed electron-nuclear double resonance (ENDOR) spectroscopy to study *in situ* the heme of CPO following inactivation with allylbenzene, using samples prepared in natural isotopic abundance, with ^{15}N-labeled enzyme, and with allylbenzene labeled with ^{2}H or ^{13}C in specific vinylic positions. These studies, in conjunction with molecular modeling (MM2) calculations, have determined the *in situ* structure of the alkene-modified heme.

Materials and Methods

Instrumentation. ^{1}H and ^{13}C NMR spectra were recorded on a General Electric QE300 with tetramethylsilane as internal standard. Fourier transform infrared spectra were recorded on a Mattson Galaxy 5000 spectrometer. Positive ion electrospray mass spectra were recorded on a Fisons VG Quattro quadrupole−hexapole−quadrupole mass spectrometer employing a flow system of 1:1 acetonitrile/water. For mass analysis of the modified hemin present in inactivated CPO following reaction with unlabeled or ^{2}H-labeled allylbenzene, samples containing 10−20 pmol/μL of CPO were denaturated by addition of 50% (v/v) acetonitrile 1−2 h prior to analysis then acidified with 0.1% (v/v) formic acid immediately before injection.

CW-EPR and ENDOR spectra were recorded at 2 K on a modified Varian E109 EPR spectrometer equipped with an E110 35 GHz microwave bridge, using 100 kHz field modulation as described elsewhere.[18] The ENDOR response was observed as a change of EPR intensity detected in the dispersion mode under condition of "rapid passage".[19] Pulsed ENDOR spectra were recorded on a locally constructed X-band (9.5 GHz)[20] and Q-band (35 GHz)[21] spectrometers, using a Mims pulsed ENDOR sequence ($\pi/2-\tau-\pi/2-T-\pi/2$).[22]

ENDOR Frequencies. The first-order ENDOR transitions for a nucleus N with spin $I = {}^1/_2$ are given by

$$\nu_{\pm} = |\nu_N \pm A^N/2| \qquad (1)$$

where ν_N and A^N are the nuclear Larmor frequency and the hyperfine coupling constant, respectively. For a nucleus with spin $I \geq 1$, the $\nu_{\pm}$ transitions will be further split into $2I$ lines by the quadrupole interaction,

$$\nu_{\pm}(m_I) = |\nu_N \pm A^N/2 + (3P^N/2)(2m_I - 1)| \qquad (2)$$

where P^N is the quadrupole coupling constant and $I \geq m_I > -I + 1$. For a frozen-solution sample with a rhombic EPR signal (g_1, g_2, g_3), the full hyperfine tensor of a hyperfine-coupled nucleus, including both the principal values and the orientation in the **g**-tensor axis frame, can be determined by analyzing the full 2-D pattern generated by collecting ENDOR spectra across the whole EPR envelope, as described elsewhere.[23]

MM2 Calculation. MM2 energy minimization was performed by using the molecular modeling and analysis program "CS Chem3D" (CambridgeSoft Co., Cambridge, MA). The program employs Allinger's MM2 force field for energy minimizations.[24] In modeling the heme structure of AB-CPO, the local geometry of Fe(III) was initially assumed to be square pyramidal. The heme nitrogens were assigned to pyrrole or ammonium nitrogen (see Results).

Materials. Phenylacetic acid-*1*-^{13}*C* (99 atom % ^{13}C) and iodomethane-^{13}*C* (99 atom % ^{13}C) were from Sigma. Lithium aluminum deuteride (96 atom % D) was from Aldrich. $Na^{15}NO_3$ (98 atom % ^{15}N) was from Cambridge Isotope Laboratories. Phenylacetaldehyde and pyridine were distilled prior to use. Tetrahydrofuran was distilled from sodium benzophenone ketyl. Dess-Martin periodinane was prepared as described.[25] Other reagents were of the highest purity available from Aldrich and were used as received. CPO was produced in cultures of *C. fumago* grown in fructose-salts medium. For preparation of uniformly ^{15}N-labeled enzyme, $Na^{15}NO_3$ was used as the sole nitrogen source in the fungal growth medium. CPO was isolated from the growth medium by two cycles of ethanol precipitation, followed by dialysis against 10 mM K^+ phosphate at pH 5.8. Ethanol−precipitated enzyme was purified further on DEAE-cellulose in a gradient of 10−300 mM K+ phosphate at pH 5.8 containing 2 mM EDTA. Native CPO purified by this method had R_Z greater than 1.45 and was substantially free of spin-active metal contaminants.

Preparation of ENDOR Samples. Allylbenzene-inactivated CPO was prepared by reacting the native enzyme with hydrogen peroxide and alkene in an aqueous emulsion. In a typical procedure, native CPO (85 mg) was added to a rapidly stirred suspension of 50 mg of allylbenzene in 20 mM K^+ acetate, pH 5.2 (40 mL). Hydrogen peroxide (1.0 mM/min) was added over 25 min until the reaction turned bright green. At this point, only trace chlorinating activity could be detected in the enzyme preparation. Further workup of the inactivated enzyme was carried out at 4 °C to slow the spontaneous reactivation. The sample was passed over a 0.25 μm syringe filter to remove particulates, exchanged three times into fresh 20 mM K^+ acetate, pH 5.2, then concentrated and frozen in ENDOR tubes and stored in liquid nitrogen. Samples to be measured in D_2O solution were prepared in H_2O buffer then exchanged six times into 20 mM K^+ acetate-d_4 at pD 5.2 in D_2O. Concentrations of allylbenzene−CPO were estimated with use of ϵ_{419} = 75 000 M^{-1} cm^{-1} and were 2−3 mM in ENDOR samples. Isotopically enriched allylbenzene−CPO was prepared as above, except that allylbenzene-*2*-*d*, allylbenzene-*1*,*1*-d_2, allylbenzene-*1*-^{13}*C*, or allylbenzene-*2*-^{13}*C* was substituted for the unlabeled alkene or ^{15}N-labeled CPO for unlabeled enzyme.

Synthesis of Labeled Allylbenzenes. Labeled allylbenzenes, except for allylbenzene-*1*-d_2, were prepared by subjecting appropriate phenylacetaldehydes to Wittig methylenation. Labeled 2-phenylethanols were made by reduction of phenylacetic acid with lithium aluminum deuteride or reduction of phenylacetic acid-*1*-^{13}*C* with lithium aluminum hydride. Alcohols were oxidized to phenylacetaldehydes with use of Dess-Martin reagent, which gave clean product nearly quantitatively. An attempt to prepare allylbenzene-*1*-d_2 with phenylacetaldehyde and $CD_2P(Ph)_3$ resulted in scrambled label. ^{1}H NMR revealed one proton attached to each of the three carbons of the allyl moiety, suggesting rapid H exchange preceding olefination. This facile enolization probably contributes to the modest yields associated with the olefination step. Synthesis of allylbenzene-*1*-d_2 was finally accomplished by to a

(18) Werst, M. M.; Davoust, C. E.; Hoffman, B. M. *J. Am. Chem. Soc.* **1991**, *113*, 1533−1538.

(19) (a) Mailer, C.; Taylor, C. P. S. *Biochim. Biophys. Acta* **1973**, *322*, 195−203. (b) Feher, G. *Phys. Rev.* **1959**, *114*, 1219−1244.

(20) Fan, C.; Doan, P. E.; Davoust, C. E.; Hoffman, B. M. *J. Magn. Reson.* **1992**, *98*, 62−72.

(21) Davoust, C. E.; Doan, P. E.; Hoffman, B. M. *J. Magn. Reson.* **1996**, *A119*, 38−44.

(22) (a) Mims, W. B. *Proc. R. Soc. London* **1965**, *A283*, 452. (b) Gemperle, C.; Schweiger, A. *Chem. Rev.* **1991**, *91*, 1481−1505.

(23) (a) Hoffman, B. M.; Gurbiel, R. J.; Werst, M. M.; Sivara, M. In *Advanced EPR. Applications in Biology and Biochemistry*; Hoff, A. J., Ed.; Elsevier: Amsterdam, 1989; pp 541−591. (b) Hoffman, B. M.; De Rose, V. J.; Doan, P. E.; Gurbiel, R. J.; Houseman, A. L. P.; Telser, J. In *EMR of Paramagnetic Molecules*; Biological *Magnetic Resonance 13*; Berliner, L. J., Reuben, J., Eds.; Plenum Press: New York, 1993; pp 151−218. (c) Hoffman, B. M. *Acc. Chem. Res.* **1991**, *24*, 164−170.

(24) (a) Burkert, U.; Allinger, N. L. *Molecular Mechanics*; American Chemical Society: Washington, DC, 1982. (b) Clark, T. C. *Computational Chemistry*; Wiley: New York, 1985.

(25) (a) Dess, D. B.; Martin, J. C. *J. Org. Chem.* **1983**, *48*, 4155−4156. (b) Ireland, R. E.; Liu, L. *J. Org. Chem.* **1993**, *58*, 2899.

modified procedure of Kwart.[26] Lithium aluminum deuteride reduction of phenylpropionic acid was followed by a three-step elimination process involving tosylation, displacement of tosylate with phenylselenide, and oxidation to a selenoxide which spontaneously eliminates.

2-Phenylethanol-*1*-d_2. Phenylacetic acid (1.00 g, 7.3 mmol) in 7 mL of THF was added slowly at room temperature and with good stirring to lithium aluminum deuteride (350 mg, 8.3 mmol) dissolved in 20 mL of THF. After 3.5 h, excess lithium aluminum deuteride was quenched by slow addition of 1 mL of methanol followed by 10 mL of 5% HCl. The mixture was diluted with ether and 10% HCl, and the layers were separated. The aqueous phase was extracted with ether, and the combined organic phases were washed with saturated $NaHCO_3$ and brine. After drying ($MgSO_4$) and removal of solvent, a colorless oil remained (0.89 g): ^{1}H NMR δ 2.85 (s, 2H, CH_2CD$_2$OH), 7.2−7.4 (m, 5H, aryl); ^{13}C NMR δ 39.0, 62.9 (pentet, J = 22 Hz), 126.4, 128.5, 129.0, 138.5; IR (thin film) 3600−3100, 2207, 2105, 1603, 1496, 1453, 1123, 1098, 744, 699 cm^{-1}.

2-Phenylethanol-*1*-^{13}*C*. The synthesis was carried out as for 2-phenylethanol-*1*-d_2, with phenylacetic acid-*1*-^{13}*C* (1.00 g) substituted for the unlabeled acid and lithium aluminum hydride substituted for the deuteride. The yield was 0.89 g: ^{1}H NMR δ 2.87 (dt, J = 5.6, 6.7 Hz, 2H, CH_2CH$_2$OH), 3.85 (dt, J = 143, 6.7 Hz, 2H, CH$_2$CH_2OH), 7.2−7.4 (m, 5H, aryl); ^{13}C NMR δ 63.6; IR (thin film) 3600−3100, 1497, 1453, 1029, 746, 699 cm^{-1}.

3-Phenylpropanol-*1*-d_2. The same procedure was used as for 2-phenylethanol-*1*-d_2, except that 3-phenylpropanoic acid (2.1 g, 14 mmol) was used instead of phenylacetic acid. Lithium aluminum deuteride (6450 mg, 15.4 mmol) was used as reductant and the reaction scaled up proportionately to give 1.87 g of product: ^{1}H NMR δ 1.90 (t, J = 7.5 Hz, 2H, PhCH_2), 2.73 (t, J = 7.5 Hz, 2H, CH_2CD$_2$OH), 7.2−7.4 (m, 5H, aryl); ^{13}C NMR δ 32.1, 34.0, 61.4 (quintet, J = 21.6 Hz), 125.9, 128.4, 128.5, 141.9; IR (thin film) 3600−3100, 2203, 2106, 1602, 1496, 1454, 1191, 1134, 1099, 965, 747, 699 cm^{-1}.

Phenylacetaldehyde-*1*-*d*. 2-Phenylethanol-*1*-d_2 (0.66 g, 5.3 mmol) in 7 mL of CH_2Cl_2 was added to Dess-Martin periodinane (2.6 g, 6.9 mmol) in 25 mL of CH_2Cl_2 and stirred for 40 min. The mixture was diluted with 100 mL of ether and poured into a mixture of saturated $NaHCO_3$ and saturated $Na_2S_2O_3$. Stirring was continued until no solid remained. The layers were separated, and the organic phase was washed with saturated $NaHCO_3$, then H_2O. After drying ($MgSO_4$), filtration through silica gel, and evaporation of solvent, a light yellow oil remained (640 mg): ^{1}H NMR δ 3.69 (s, 2H, PhCH_2), 7.2−7.4 (m, 5H, aryl).

Phenylacetaldehyde-*1*-^{13}*C*. A scaled-up procedure as for phenylacetaldehyde-*1*-*d* was used. 2-Phenylethanol-*1*-^{13}*C* (0.85 g) gave a yellow oil quantitatively (0.83 g): ^{1}H NMR δ 3.70 (dd, J = 2.3, 7.4 Hz, 2H, PhCH_2), 7.2−7.4 (m, 5H, aryl), 9.75 (dt, J = 2.3, 176 Hz, 1H, CH$_2$C*H*O); ^{13}C NMR δ 199.5; IR (thin film) 2819, 1683, 1498, 1454, 749, 700 cm^{-1}.

Allylbenzene-*2*-*d*. To methyltriphenylphosphonium bromide (2.34 g, 6.5 mmol) and potassium *tert*-butoxide (0.67 g, 6.0 mmol) under nitrogen was added 20 mL of THF. After the mixture was stirred for 30 min at room temperature, phenylacetaldehyde-*1*-*d* (0.64 g, 5.3 mmol) in 3 mL of THF was added dropwise. Stirring was continued for 1 h, excess phosphorane was quenched with silica gel, and the mixture was filtered. The filtrate was concentrated and diluted with pentane, and the triphenylphosphonium oxide precipitate was removed by filtration. The filtrate was allowed to stand overnight at 4 °C to complete precipitation, the supernatant was decanted, solvent was evaporated, and the residue was distilled in an Aldrich Quick-distill apparatus to give the pure alkene (170 mg, 24% overall yield): ^{1}H NMR δ 3.41 (s, 2H, PhCH_2), 5.09 (s, 2H, CH═CH_2), 7.2−7.4 (m, 5H, aryl); ^{13}C NMR δ 40.2, 115.7, 126.1, 128.5, 128.6, 137.2 (t, J = 24.2 Hz), 140.1; IR (thin film) 3082, 3064, 3028, 2903, 1622, 1602, 1495, 1453, 1432, 1076, 1030, 915, 842, 740, 698 cm^{-1}.

Allylbenzene-*2*-^{13}*C*. To methyltriphenylphosphonium bromide (2.83 g, 7.9 mmol) and potassium *tert*-butoxide (0.89 g, 7.9 mmol) under nitrogen was added 20 mL of THF. After the mixture was stirred for 30 min at room temperature, phenylacetaldehyde-*1*-^{13}*C* (0.80 g, 6.6 mmol) in 3 mL of THF was added dropwise. Stirring was continued for 1 h, after which the excess phosphorane was quenched with H_2O. The mixture was diluted with 25 mL of ether, and the layers were separated. The aqueous layer was extracted with fresh ether, and the combined ether layers were washed with brine, dried ($MgSO_4$), and concentrated. The residue was diluted with pentane, and triphenylphosphonium oxide was removed by filtration. After the mixture was chilled overnight at 4 °C to complete precipitation, the supernatant was decanted, the solvent was evaporated, and the remaining oil was flash chromatographed on 50 g of silica with pentane as eluant. After removal of solvent, 380 mg of pure alkene (46% overall yield) was obtained: ^{1}H NMR δ 3.41 (dd, J = 6.7, 7.6 Hz, 2H, PhCH_2), 5.07−5.13 (overlapping multiplets, 2H, CH═CH_2), 5.98 (dm, J = 154 Hz, 1H, C*H*═CH$_2$), 7.2−7.4 (m, 5H, aryl); ^{13}C NMR δ 137.4; IR (thin film) 1612, 1602, 1495, 1453, 1432, 990, 913, 740, 698 cm^{-1}.

Allylbenzene-*1*-^{13}*C*. Triphenylphosphine (1.8 g, 7.0 mmol) was dissolved in 5 mL of ether, and iodomethane-^{13}*C* (1.0 g, 7.0 mmol) was added. After 24 h in a sealed flask at room temperature, 2.65 g (93%) methyltriphenylphosphonium iodide was collected by filtration. This labeled phosphonium salt was treated with phenylacetaldehyde (0.7 mL) and potassium *tert*-butoxide (0.66 g) in a manner identical with the preparation of allylbenzene-*2*-^{13}*C* to give 100 mg (14% overall yield) of product. ^{1}H NMR δ 3.41 (dd, J = 6.2, 6.1 Hz, 2H, PhCH_2), 5.07−5.13 (dm, J = 156 Hz, 2H, CH═CH_2), 6.00 (m, 1H, C*H*═CH$_2$), 7.2−7.4 (m, 5H, aryl); ^{13}C NMR δ 115.8; IR (thin film) 1617, 1602, 1495, 1453, 1432, 1030, 994, 906, 740, 698 cm^{-1}.

Allylbenzene-*1*-d_2. Crude 3-phenylpropanol-*1*-d_2 prepared above was dissolved in 10 mL of CH_2Cl_2. *p*-Toluenesulfonyl chloride (2.9 g, 15.4 mmol) and pyridine (1.22 g, 15.4 mmol) were added. After being stirred at room temperature for 65 h, the reaction mixture was diluted with 70 mL of ether and extracted sequentially with 10 mL of H_2O and 10 mL of 10% HCl. The organic solution was stirred vigorously with 25 mL of concentrated NH_4OH for 1 h until TLC revealed that the excess tosyl chloride had reacted. The layers were separated, the organic layer was extracted sequentially with 2 N NaOH, H_2O, and brine dried ($MgSO_4$), and the solvent was evaporated to give 3.1 g of colorless oil. Diphenyl diselenide (2.26 g, 7.2 mmol) was dissolved in 40 mL of ethanol, and sodium borohydride (0.53 g, 14.0 mmol) was spooned in portionwise. After the mixture was cooled to 0 °C, the tosylate-d_2 in 30 mL of THF was added. The reaction mixture was warmed to room temperature and stirred for 4 h before being poured into 5% K_2CO_3. Extraction with ether, drying ($MgSO_4$), and removal of solvent gave 3.1 g of crude selenide as a yellow oil. The residue was taken up into 30 mL of CH_2Cl_2, and cumene hydroperoxide (2.04 g, 1.0 equiv based on 80% tech grade) was added. After 24 h of stirring at room temperature, the mixture was diluted with an equal volume of pentane and filtered through silica gel. The solvent was stripped, and flash chromatography (42 g of silica gel, pentane) was performed to give 340 mg of colorless oil. ^{1}H NMR revealed minor contamination by cumene, but this did not interfere with the use of allylbenzene-*1*-d_2 for enzyme reactions: ^{1}H NMR δ 3.43 (d, J = 6.7 Hz, 2H, PhCH_2), 6.00 (broad m, 1H, C*H*═CH$_2$), 7.2−7.4 (m, 5H, aryl); ^{13}C NMR δ 40.2, 126.1, 128.4, 128.6, 137.3, 140.1.

Results

Mass Analysis of Allylbenzene-Modified Heme. When AB-CPO is denatured with acetonitrile and analyzed by electrospray MS, the major low molecular weight (i.e. non-protein) component is observed at m/z 750.4.[7] From the half-integer spacing of isotope peaks, this metalloporphyrin species is deduced to be doubly charged and hence, dimeric. This species most likely represents a μ-oxo dimer of the modified hemin. Formation of μ-oxo dimers from model *N*-alkylhemins has been reported elsewhere.[27] The formation of this dimer appears to be facile not only under electrospray MS conditions but also in larger-scale extractions. As extracted from AB-CPO, the

(26) Kwart, H.; Brechbiel, M.; Miles, W.; Kuart, L. D. *J. Org. Chem.* **1982**, *47*, 4524−28.

(27) (a) Wyslouch, A.; Latos-Grazynski, L.; Grzeszczuk, M.; Drabent, K.; Bartczak, T. *J. Chem. Soc., Chem. Commun.* **1988**, 1377−1378. (b) Bartczak, T. J.; Latos-Grazynski, L.; Wyslouch, A. *Inorg. Chim. Acta* **1990**, *171*, 205−212.

dimeric hemin is EPR-silent and exhibits broad electronic absorption bands at 408, 504, and 596 nm (Dexter, A. F.; Xia, Y.-M.; Debrunner, P. G. Unpublished data). The mass change of the modified hemin relative to heme b ($m/z = +134$ per monomer) corresponds to the addition of allylbenzene plus an oxygen atom, consistent with previous studies on alkene-mediated heme modification. When allylbenzene-*2-d* is used instead of the unlabeled alkene, the mass spectrum of the porphyrin dimer has maximum intensity at m/z 751.4 ($m/z = +1$ per monomer), indicating retention of the ^{2}H label (data not shown). With allylbenzene-*1,1-d*$_2$, the maximum peak intensity shifts to m/z 752.4, indicating retention of both vinylic deuterons. Hence, all three vinylic protons of allylbenzene are retained in the modified hemin.

EPR. The CW-EPR spectrum of native CPO at pH 5.2 in low-temperature frozen solutions exhibits a rhombic, low-spin ferric signal with $g_{1,2,3} = 2.61$, 2.26, and 1.84.[28] Sono *et al.* carried out extensive EPR studies showing that this signal corresponds to a heme center with a thiolate ligand,[29a] a result also suggested by other spectroscopic methods.[29b,c] The presence of a proximal cysteine thiolate in CPO was confirmed by the recent crystal structure.[30] In the crystal structure, determined at room temperature, the iron is displaced by 0.14 Å out of the heme plane toward the thiolate ligand, and a water molecule is positioned 3.4 Å from the iron on the distal site of the heme, beyond bonding distance. This is consistent with the observed high-spin properties of CPO at room temperature. At lower temperatures, CPO undergoes a transition to a low-spin six-coordinate form. ^{1}H ENDOR studies have shown that the low-spin CPO has a solvent water as a second axial ligand, thus demonstrating that the hemes of low-spin CPO and P450 share the same coordination.[31] Following inactivation of CPO with allylbenzene, the EPR signal of native CPO disappears a new low-spin rhombic EPR signal appears with substantially smaller g spread ($g_{1,2,3} = 2.32$, 2.16, 1.95).

As will be seen below, determination of the metrical parameters that describe the structure of the heme moiety of AB-CPO requires a knowledge of the orientation of the **g**-tensor axes relative to the heme plane. In general, the g_1 axis of a low-spin ferric heme is normal to the heme plane and g_2 and g_3 axes are in the plane.[32] As this has been experimentally verified for the similar, cysteine-bound heme of P450,[31] we may assume the same for CPO and AB-CPO. This leaves to be determined the rotation (angle ϕ) of the g_2, g_3 axes about the g_1 axis, relative to the heme frame, namely relative to the Fe−N (pyrrole) bonds (Figure 1). The solution to this question was obtained from ENDOR studies of [^{14,15}N]AB-CPO.

ENDOR of [^{14,15}N]Allylbenzene−CPO. Single crystal-like ENDOR spectra of [^{14,15}N]AB-CPO collected at the low-field (g_1) and high-field (g_3) edges of the EPR envelope are compared in Figure 2. In the figure, only ν_+ branches are shown; the ν_- branches are expected to fall near 1 MHz and are very difficult to detect. In the ^{15}N spectra at g_1 and g_3, four distinct ν_+ peaks, assigned to the four ^{15}N pyrrole nitrogens, are observed. One nitrogen, denoted N_a, has a hyperfine coupling of less than 5 MHz; each of the others, denoted N_{b-d}, has a coupling greater than 7 MHz (Table 1). The hyperfine values for the second group are similar to those observed in ^{15}N ENDOR of the pyrrole nitrogens in native CPO, where the four pyrroles gave rise to three resolvable ^{15}N ENDOR peaks with hyperfine couplings of 7.0, 7.9, and 8.7 MHz at g_1 (data not shown). The *ca.* 40% reduction in the hyperfine coupling to N_a upon allylbenzene inactivation, contrasted with the invariance of the couplings to N_{b-d}, does not support a structure in which the alkene fragment binds only to Fe (**5**, **6**), and instead strongly suggests one in which the alkene fragment is directly bonded to N_a of the AB-CPO heme (**2**−**4**).

Comparison of the ^{14}N ($I = 1$) and ^{15}N ($I = {}^1/_2$) ENDOR spectra of AB-CPO in Figure 2 permits an analysis of the

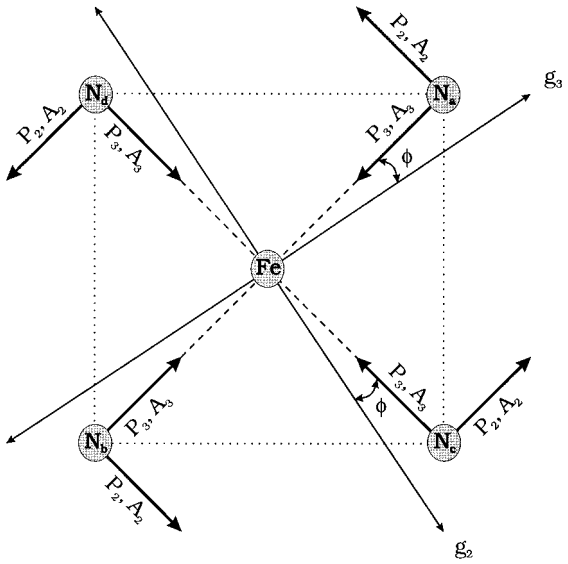

Figure 1. Definition of the angle ϕ and of the directions of the pyrrole−nitrogen hyperfine and quadrupole tensors with respect to an idealized heme plane, which includes g_2 and g_3 axes.

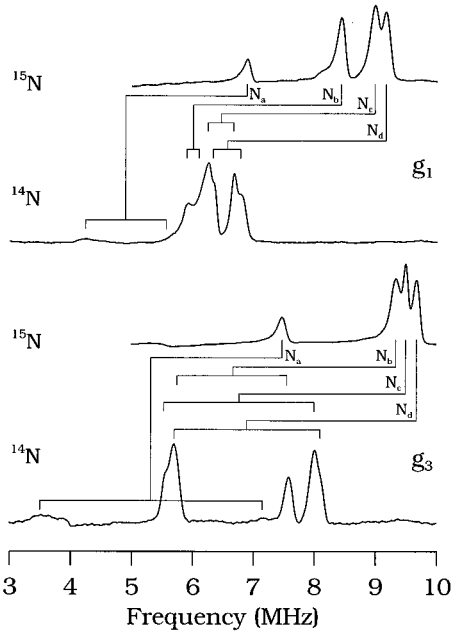

Figure 2. Q-band ^{14,15}N CW-ENDOR spectra taken at the low-field ($g_1 = 2.32$) and the high-field ($g_3 = 1.95$) edges of the EPR envelopes of the naturally abundant and ^{15}N-enriched AB-CPO samples. Experimental conditions: microwave frequency, 35.00 (^{15}N), 34.97 (^{14}N) GHz; modulation amplitude, 1.3 G; RF sweep, 0.4 (^{15}N), 0.5 (^{14}N) MHz/s. ^{14}N quadrupole splittings are indicated by a "goal post", and corresponding ^{15}N's are connected by solid lines.

(28) Hollenberg, P. F.; Hager, L. P.; Blumberg, W. E.; Peisach, J. *J. Biol. Chem.* **1980**, *255*, 4801−4807.

(29) (a) Sono, M.; Hager, L. P.; Dawson, J. H. *Biochim. Biophys. Acta* **1991**, *1078*, 351−359. (b) Dawson, J. H.; Sono, M. *Chem. Rev.* **1987**, *87*, 1255−1276. (c) Yarmola, E. G.; Sharonov, Y. A. *FEBS Lett.* **1994**, *35*, 279−281.

(30) Sundaramoorthy, M.; Terner, J.; Poulos, T. L. *Structure* **1995**, *3*, 1367−1377.

(31) Fann, Y. C.; Gerber, N. C.; Osmulski, P. A.; Hager, L. P.; Sligar, S. G.; Hoffman, B. M. *J. Am. Chem. Soc.* **1994**, *116*, 5989−5990.

(32) Murray, R. I.; Fisher, M. T.; Debrunner, P. G.; Sligar, S. G. In *Metalloproteins. Part 1: Metal Proteins with Redox Roles*; Harrison, P. M., Ed.; Verlag Chemie: Florida, Basel, 1985; Chapter 5, pp 157−206.

Table 1. ^{15}N Hyperfine Tensors and ^{14}N Nuclear Quadrupole Tensors of the Heme Nitrogens of Allylbenzene−CPO[a]

	^{15}N hyperfine tensors (MHz)				^{14}N nuclear quadrupole tensors (MHz)				
nucleus	A_1	A_2	A_3	ϕ^b (deg)	P_1	$P(g_3)^c$	ϕ^b (deg)	$P_3{}^d$	$P_2{}^e$
N_a	4.6	4.1	3.7	0−20[f]	0.43	−1.20	*g*	*g*	*g*
N_b	7.6	7.6	7.6	0[g]	0.06	−0.6	10−20	−0.68	0.62
N_c	8.7	7.9	7.3	∼0[g]	0.17	−0.8	10−20	−1.12	0.97
N_d	9.0	8.3	7.5	∼0[g]	0.17	−0.8	10−20	−1.12	0.97

[a] The tensor principal values (A_i, P_i) are defined in the local tensor frame (see Figure 1). Uncertainties for A_i, ±0.15 MHz, and uncertainties for P_i, ±0.1 MHz, are based on uncertainties of ±5° in ϕ. [b] The angle is defined in Figure 1. [c] The measured value along g_3. [d] Calculated from P_1, $P(g_3)$, and $\phi = 15°$ through use of eqs 3 and 4 (see text). [e] Calculated from P_1, P_3, and the constraint $P_1 + P_2 + P_3 = 0$. [f] The fit also suggests that A_3 is ∼25° out of the g_2, g_3 plane (heme plane). [g] Not well defined.

quadrupole splittings for the former. The ^{14}N hyperfine couplings are simply obtained by the ratio of the nuclear *g* factors, $|A(^{15}N)/A(^{14}N)| = |g(^{15}N)/g(^{14}N)| = 1.403$, while, as indicated in the figure, each $\nu_+(^{15}N)$ feature becomes a quadrupole-split ^{14}N doublet. As with the hyperfine interaction, the quadrupole splitting of N_a is significantly different from those of the pyrrole $^{14}N_{b-d}$ at g_1 (Table 1). This confirms that the nitrogen, N_a, is significantly altered by the addition of allylbenzene and supports the conclusion that allylbenzene binds to N_a. Among the pyrrole nitrogens, N_{b-d}, N_c, and N_d have the same quadrupole coupling constants while N_b has a different value. Based on this observation, we provisionally assign N_b as *trans* to the unique nitrogen, N_a.

In a "normal" heme, the orientation of the **g** tensor can be deduced from its orientation relative to the hyperfine tensors of the pyrrole nitrogens, because the latter normally can be taken to have principal axes that include the Fe−N bond and the out-of-plane (g_1) normal to it.[33] To this end, ^{15}N ENDOR spectra were collected across the EPR envelope, and this 2-D set of orientation-selective spectra was analyzed as described elsewhere.[23] For $^{15}N_{b,c,d}$ the hyperfine anisotropy is very small and the signals are strongly overlapped. It was possible to estimate principal values for the N_{b-d} tensors (Table 1) by assuming the coincidence of the hyperfine- and **g**-tensor axes, namely rotation angle $\phi = 0°$ of the Fe−N framework relative to the **g**-tensor axes; a reliable limit on deviations from zero could not be determined. The signal for N_a is well resolved, however, and simulation of the field dependence of the $^{15}N_a$ ENDOR spectra (data not shown) indicates that the tensor axes are rotated by an angle of $\phi \leq 20°$ about the g_1 axis (Table 1, see Figure 1). This orientation of the **g** tensor relative to the heme plane is quite comparable to that directly determined for native P450 by single-crystal EPR measurements where $\phi = 18°$.[32]

The above result was further tested because bonding of allylbenzene to N_a might produce distortions of the heme that cause the principal axis of the N_a hyperfine tensor not to lie along the metal−nitrogen bond in AB-CPO. The results was confirmed, and the best estimate for ϕ was obtained, by considering the ^{14}N quadrupole interactions for the *unperturbed*, b−d, pyrrole nitrogens. The small anisotropy of the ^{15}N hyperfine tensors translates to an even smaller anisotropy for ^{14}N. As a result, the field dependence of the $^{14}N_{b-d}$ ENDOR spectra is almost completely determined by the quadrupole interaction. Earlier studies showed that the axis of the maximum nuclear quadrupole coupling (P_3) for a pyrrole ^{14}N lies along the metal−nitrogen bond and the smallest coupling (P_1) is along the normal to heme, that is the g_1 axis (see Figure 1).[34] Hence, a determination of the orientation of the pyrrole quadrupole tensors through an analysis of the field-dependent $^{14}N_{b-d}$ ENDOR spectra yields the angle ϕ by which the **g** tensor is rotated about g_1.

The analysis for a pyrrole ^{14}N begins by taking advantage of the fact that the quadrupole tensor is traceless, $P_1 + P_2 + P_3 = 0$, which reduces the number of unknowns from four (three P_i plus ϕ) to three. The quadrupole splittings in the ENDOR spectrum taken at g_1 (Figure 2) give $3P_1(N_b, N_c, N_d) = (0.2, 0.5, 0.5$ MHz), leaving two unknowns which we take as the angle ϕ and the largest principal value P_3. The nuclear quadrupole splitting measured at g_3, $3P(g_3; N_b, N_c, N_d) = (1.8, 2.4,$ and 2.4 Mhz), can then be incorporated into a relationship between ϕ and P_3 for each of N_b-N_d. It can be written for N_b as

$$\cos^2\phi = [P(g_3, N_b) - P_1(N_b) - P_3(N_b)]/[P_1(N_b) + 2P_3(N_b)] \quad (3)$$

and for N_c and N_d as

$$\sin^2\phi = [P(g_3, N_{c,d}) - P_1(N_{c,d}) - P_3(N_{c,d})]/[P_1(N_{c,d}) + 2P_3(N_{c,d})] \quad (4)$$

^{14}N ENDOR spectra for N_{b-d} were calculated for fields across the EPR envelope of AB-CPO through use of the hyperfine couplings as scaled from the ^{15}N values, the measured P_1, and for values of ϕ within the physically significant range, $0° \leq \phi \leq 45°$; the above relationships were then used to calculate P_3. Comparison of the simulations to experimental spectra (data not shown) confirmed that the angle between Fe−N_a (N_a-N_b) and g_3 is less than 20°; in particular, when the angle is taken to be greater, the total breadth of the ENDOR pattern simulated for $g = g_2$ is greater than that seen in the experimental data. Overall, simulations of the ^{14}N data (not shown) indicate that the **g** tensor is rotated about the g_1 (heme normal) axis by an angle of $\phi = 15° \pm 5°$ (Figure 1), in good agreement with the value of $\phi \leq 20°$ estimated from the analysis of the $^{15}N_a$ hyperfine tensor. This result lays the foundation for analysis of the following ^{1,2}H ENDOR analysis of the structure of the heme-bound allylbenzene.

^{13}C ENDOR of Allylbenzene−CPO with ^{13}C-Labeled Allylbenzene. Well-resolved ^{13}C ENDOR signals not visible for natural-abundance samples are observed in spectra of *both* AB-*1*-^{13}*C*-CPO and AB-*2*-^{13}*C*-CPO, as seen in data taken at the low-field edge (g_1) of the Ab-CPO EPR spectrum, Figure 3. This confirms that the allylbenzene framework is preserved in AB-CPO. Somewhat surprisingly, the hyperfine couplings in these spectra are comparable for the two locations ($A(^{13}$C-1, ^{13}C-2) ∼ 3 MHz). However, field-dependent ^{13}C ENDOR studies (data not shown) reveal a slightly larger maximum component for ^{13}C-2 (∼5 MHz vs ∼ 4 MHz), and while both tensors are dominated by the isotropic contribution, the dipolar term is more significant for ^{13}C-2.

^{1}H ENDOR of Allylbenzene−CPO in H_2O and D_2O. The ^{1}H ENDOR spectra of AB-CPO in H_2O and D_2O buffers collected at the low-field edge (g_1) of the EPR envelope are compared in Figure 4, parts A and B. ^{1}H ENDOR from the sample in H_2O buffer (Figure 4A) shows intensity with $A \leq 5$ MHz and one strongly coupled proton with the hyperfine

(33) (a) Brown, T. G.; Hoffman, B. M. *Mol. Phys.* **1980**, *39*, 1073−1109. (b) Scholes, C. P.; Lapidot, A.; Mascarenhas, R.; Inubushi, T.; Isaacson, R. A.; Feher, G. *J. Am. Chem. Soc.* **1982**, *104*, 2724−2735.

(34) (a) Hsieh, Y. N.; Rubenacker, G. V.; Cheng, C. P.; Brown, T. L. *J. Am. Chem. Soc.* **1977**, *99*, 1384−1389. (b) Ashby, C. I. H.; Cheng, C. P.; Brown, T. L. *J. Am. Chem. Soc.* **1978**, *100*, 6057−6063. (c) Ashby, C. I. H.; Cheng, C. P.; Duelsler, E. N.; Brown, T. L. *J. Chem. Soc.* **1978**, *100*, 6063−6067.

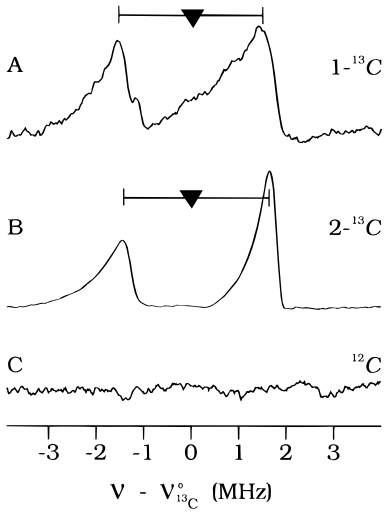

Figure 3. Q-band ^{13}C CW-ENDOR spectra taken at the low-field edges ($g_1 = 2.32$) of the EPR envelopes of AB-CPO samples with ^{13}C labeled at the allylbenzene C-1 (A) and C-2 (B) positions and (C) from naturally abundant allylbenzene. Experimental conditions: microwave frequency, 35.06 (A), 35.06 (B), 35.17 (C) GHz; modulation amplitude, 1.3 G; RF sweep, 0.5 MHz/s. All spectra are centered at ^{13}C Larmor frequency marked by ▼.

coupling of 24 MHz as indicated by the "goal-post" mark. It should be noted that in Q-band ENDOR one often sees unequal intensity of the ν_+ and ν_- branches of a doublet; here ν_+ appears with an opposite phase. Figure 4B shows that this doublet persists in D_2O buffer. The reduced intensity of the ν_+ signal intensity of the 24 MHz coupled doublet is assigned to changes in nuclear spin relaxation, not to a proton exchange.

The absence of the exchangeable protons found in native CPO implies that the axial H_xO^{x-2} ($x = 1$ or 2) ligand of the native CPO is replaced in AB-CPO.[31] The strongly coupled, non-exchangeable proton ($A(^1H) = 24$ MHz) might arise either from β-protons of the cysteinyl thiolate proximal ligand or from a site on the allylbenzene substrate. To resolve this issue, as well as to probe structural details of the AB-modified hemin, we synthesized allylbenzene (**7**) specifically labeled with ^2H in the two vinylic positions (allylbenzene-*1,1-d*$_2$, allylbenzene-*2-d*) and prepared ENDOR samples from CPO inactivated with each of the labeled alkenes.

^{1,2}H ENDOR of Allylbenzene-*2-d*−CPO. The ^1H and ^2H ENDOR spectra of AB-*2-d*-CPO at g_1 are displayed in Figure 4, parts C and D. The ^1H signal with the hyperfine coupling of 24 MHz (Figure 4A,B) disappears for AB-*2-d*-CPO (Figure 4C). The corresponding ^2H ENDOR signal (Figure 4D) appears as a doublet split by the hyperfine coupling of $A(^2H) = 3.8$ MHz as expected from the Larmor ratio, $|\nu(^1H)/\nu(^2H)| = |A(^1H)/A(^2H)| = 6.51$. This result confirms that the vinylic proton of allylbenzene is present in the modified hemin *in situ*.

Analysis of the full field-dependent ^1H ENDOR pattern of AB-CPO across the EPR envelope reveals that the hyperfine coupling of the proton on the C-2 position (denoted H_{2a}) of AB-CPO is mostly isotropic, with tensor values of $A = (24.6, 17.0, 16.2)$ MHz. A glance at the spectrum shows that any signal from a proton on the C-1 position must fall within the central feature, and cannot have a ^1H hyperfine splitting greater than *ca.* 5−6 MHz at any field. This sharp disparity in the couplings to the two types of protons implies that the heme of AB-CPO must adopt a structure in which C-2 retains its bond to the hydrogen and is closer to Fe(III) than C-1. Of structures **2**−**6**, only **2** satisfies this description, provided R = CH_2Ph and R′ = H.

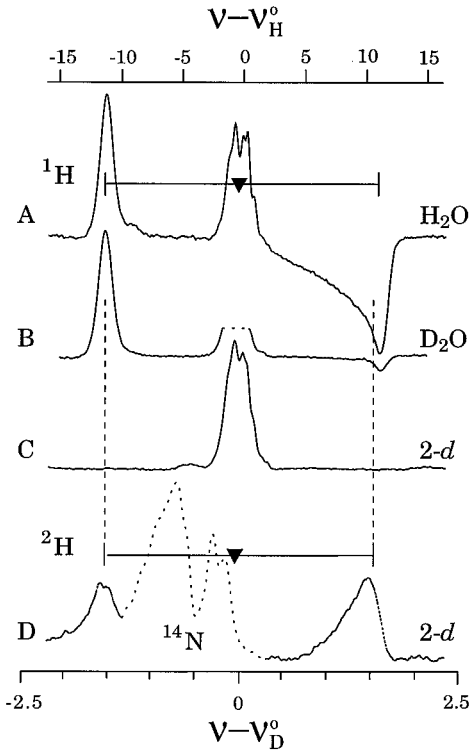

Figure 4. Q-band ^1H [(A) AB-CPO in H_2O; (B) AB-CPO in D_2O; (C) AB-*2-d*-CPO] and ^2H [(D) AB-*2-d*-CPO] CW-ENDOR spectra taken at the low-field edge ($g_1 = 2.32$) of each EPR envelope. Experimental conditions: microwave frequency, 35.17 (A), 35.42 (B), 35.30 (C, D) GHz; modulation amplitude, 0.7 (A, B, C), 1.3 (D) G; RF sweep, 2.0 (A, B, C), 0.5 (D) MHz/s. The dotted line in part D represents ^{14}N resonances, and all spectra are centered at each Larmor frequency marked by ▼. The frequency of the ^2H spectrum (D) is scaled (×6.51) to match those of ^1H spectra.

^{1,2}H ENDOR of Allylbenzene-*1,1-d*$_2$−CPO. The presence of structure **2** and the inferred orientation of the alkylbenzene is confirmed, and indeed a detailed structure of the heme moiety in AB-CPO is obtained, by examining the signals from the hydrogens attached to the C-1 position of allylbenzene. The ^1H (C-1) signals are best seen in the difference ^1H ENDOR spectra obtained by subtracting the ^1H ENDOR of AB-*1,1-d*$_2$-CPO from those of AB-CPO, Figure 5A. In the figure, the dashed lines represent one proton (denoted H_{1a}); as will be explained, the solid lines represent the other proton (denoted H_{1b}). The pattern of the $^1H_{1a}$ resonances that emerge in the 2-D display of spectra taken across the EPR envelope is typical for a proton whose hyperfine coupling is dominated by dipolar coupling to the spin on the ferric ion. As illustrated in Figure 5B, the pattern is well simulated by an almost purely dipolar tensor, with components $\mathbf{A} = [-2.8, -2.8, 5.0]$ MHz $= -0.2 + [-2.6, -2.6, 5.2]$ MHz; here, the signs are fixed by the fact that the interaction is governed by the through-space dipolar coupling, the isotropic coupling is $a = -0.2$ MHz, and the $[Fe^{III}-H_{1a}]$ distance within the point-dipole approximation is $d = 3.1$ Å. The $Fe-H_{1a}$ vector corresponds to the unique axis of the $^1H_{1a}$ tensor, A_3, and the orientation of this axis with respect to **g**-tensor frame (Euler angle: $\phi(H_{1a}) = 7°$; $\theta(H_{1a}) = 56°$) corresponds to the orientation of the proton in the **g**-tensor frame. The results of the $^{14,15}N$ ENDOR measurements then can be used to orient H_{1a} relative to the heme plane as shown in Figure 6. This figure has assumed a particular resolution of the one ambiguity in describing the projection of the $Fe^{III} \rightarrow H_{1a}$ vector, $\mathbf{d}(H_{1a})$, onto the heme plane, as is better illustrated in Figure 6B. The ambiguity is that the **g** tensor is rotated relative to the heme frame by $\phi(\mathbf{g}) = 15°$ about g_1, and the $\mathbf{A}(H_{1a})$ tensor is

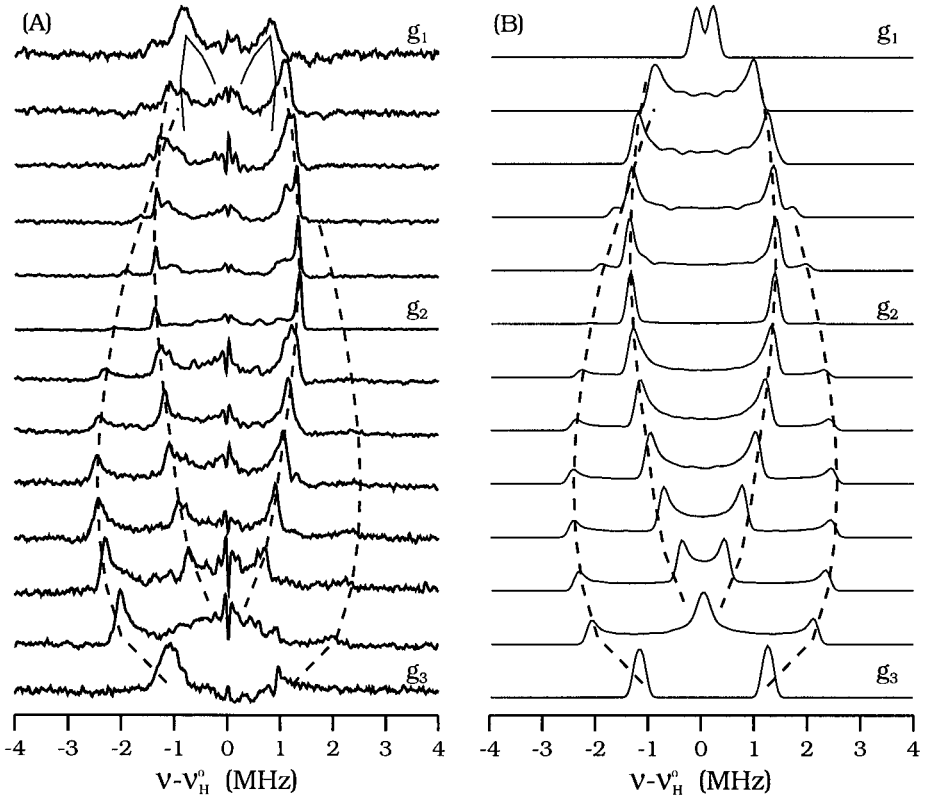

Figure 5. (A) ^{1}H ENDOR spectra calculated by subtracting the Q-band ^{1}H CW-ENDOR of AB-*1,1-d*$_2$-CPO from those of AB-CPO. Experimental conditions: microwave frequency, 35.04 GHz; modulation amplitude, 1.3 G; RF sweep, 0.5 MHz/s. The dotted lines indicate the proton denoted as H_{1a} while the solid lines indicate the proton denoted as H_{1b} (see text). (B) ^{1}H ENDOR simulation with $\mathbf{A} = [-2.8, -2.8, 5.0]$ MHz, Euler angles of $\theta = 56°$ and $\phi = 7°$, and ENDOR line width of 0.2 MHz. Here, **A** is the hyperfine tensor. All the spectra are centered at ^{1}H Larmor frequency.

rotated relative to the **g** frame by $\phi(H_{1a}) = 7°$ about g_1, but the relative signs of these angles is not fixed. Thus, the angle between the projection of $\mathbf{d}(H_{1a})$ and the $Fe^{III}-N_a$ vector can be either 8° or 22°, depending on whether the two ϕ angles have the opposite or same signs. For reasons that will become clear, Figure 6 assumes they have opposite signs.

Figure 5 showed one proton (H_{1a}) on the C-1 position of the allylbenzene adduct. The mass spectrum indicates that both C-1 protons are present, but signals from the second one (H_{1b}) are not evident in these ^{1}H CW-ENDOR spectra. The second hydrogen, H_{1b}, instead was detected in ^{2}H Q-band Mims ENDOR spectra of allylbenzene-*1,1-d*$_2$-CPO (Figure 7). The ^{2}H measurement at Q-band has no background and is specially useful for detecting weak hyperfine couplings. The experimental data represented by thin lines are the ^{2}H ENDOR signal of the deuteron (D_{1a}) corresponding to H_{1a}. They show ν_+ and ν_- branches at each field separated by ~0.45 MHz, as expected by the Larmor ratio $|\nu(^1H)/\nu(^2H)| = |A(^1H)/A(^2H)| = 6.51$; each branch is further split by the nuclear quadrupole interaction. The simulation for D_{1a} is seen as solid lines where the ^{2}H hyperfine tensor is determined from ^{1}H tensor and the nuclear *g* factors. The features depicted by thicker solid lines in Figure 7 are not predicted for the deuteron, D_{1a}, and are from the second deuteron, D_{1b}, in AB-*1,1-d*$_2$-CPO. The simulations for D_{1b}, with the hyperfine coupling of $\mathbf{A} = [-0.29, -0.29, 0.49]$ MHz and the Euler angle = [36°, 71°, 0°] with respect to the **g**-tensor frame, are shown as dashed lines. The corresponding H_{1b} hyperfine tensor is $\mathbf{A} = [-1.9, -1.9, 3.2]$ MHz. The isotropic coupling constant of $^1H_{1b}$ is $a = -0.2$ MHz, the same as for $^1H_{1a}$, within the point-dipole approximation the $[Fe^{III}-H_{1b}]$ distance is $d = 3.6$ Å. From the hyperfine coupling and Euler angle determined by ^{2}H ENDOR of D_{1b}, H_{1b} can be positioned in the heme plane as well as the **g**-tensor frame as in Figure 6,

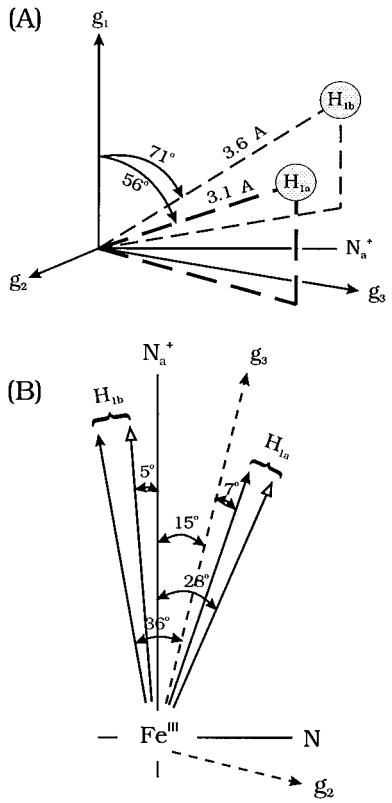

Figure 6. (A) ENDOR-determined orientation of N_a^+, H_{1a}, and H_{1b} (see text). The ENDOR measurement determines $|\phi|$. Of the two possibilities, one orientation is chosen for each with the aid of the MM2 calculation. (B) ENDOR (solid arrowhead) and MM2 (open arrowhead) determined orientations of **g**-tensor axes and C-1 protons as projected on the heme plane containing Fe(III) and pyrrole nitrogens.

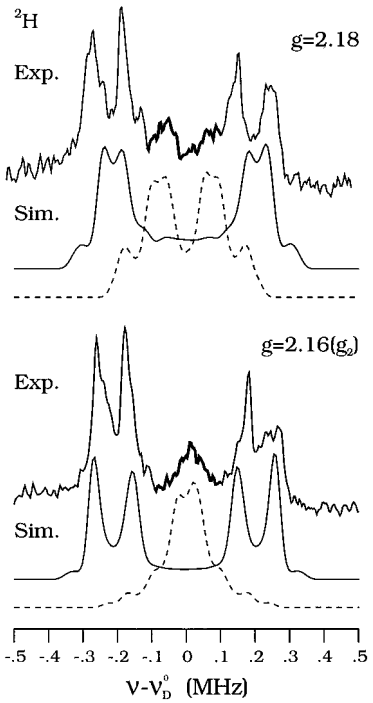

Figure 7. Q-band ^{2}H Mims ENDOR spectra of AB-*1,1-d*$_2$-CPO. Experimental Conditions: τ, 1300 ns; repetition rate, 50 Hz; RF pulse width, 60 μs; average, 580 transients at $g = 2.18$, 480 transients at $g = 2.16$. Experimental data represented by a thicker line indicate D_{1b} while a thinner line represents D_{1a}. The simulation displayed by a solid line is for D_{1a} and that represented by a dotted line is for D_{1b}. Simulation parameters for D_{1a} are $\mathbf{A} = [-0.43, -0.43, 0.77]$ MHz, $\theta_A = 56°$, $\phi_A = 7°$, $\mathbf{P} = [-0.0275, -0.0275, -0.0550]$ MHz, $\theta_P = 76°$, $\phi_p = 69°$; for D_{1b} $\mathbf{A} = [-0.29, -0.29, 0.49]$ MHz, $\theta_A = 71°$, $\phi_A = 36°$, $\mathbf{P} = [-0.0275, -0.0275, -0.0550]$ MHz, $\theta_P = 77°$, $\phi_p = 38°$. Here, **A** is the hyperfine tensor and **P** is the nuclear quadrupole tensor.

again with a particular resolution of an ambiguity analogous to the one for H_{1a}.

Structure of the Allylbenzene-Modified Hemin. The results of the ENDOR studies and mass analysis are sufficient to distinguish between structures **2**−**6** for the hemin present in AB-CPO. First, the observation of a ferric EPR signal is sufficient to rule out the carbene **5**. Although stable iron(II) carbenes (PFe^{IV}=CRR′ ↔ PFe^{II} ← CRR′) are known, both in enzyme and model hemin systems,[35] one-electron oxidation of these carbenes leads to the formation of an Fe,N bridged ferric species similar to **4**,[8] not a stable iron(III) carbene. The heme of AB-CPO thus cannot be formulated as a β-hydroxycarbene. Second, ^{14,15}N ENDOR data show that one of the four pyrrole nitrogens of AB-CPO has distinctive hyperfine and nuclear quadrupole couplings. These suggests modification of the heme at one of the pyrrole rings, consistent with structures **2**−**4** but not the carbene **5** or the σ-alkyl species **6**.

The N-alkylated structures **2**−**4** are distinguished by the ^{1,2}H ENDOR of AB-CPO and deuterated AB-CPO. The experiments reveal different types of proton hyperfine interaction for protons on the C-1 position and C-2 position of allylbenzene. The coupling for H_{2a} (C-2 position) is strong and mostly isotropic,

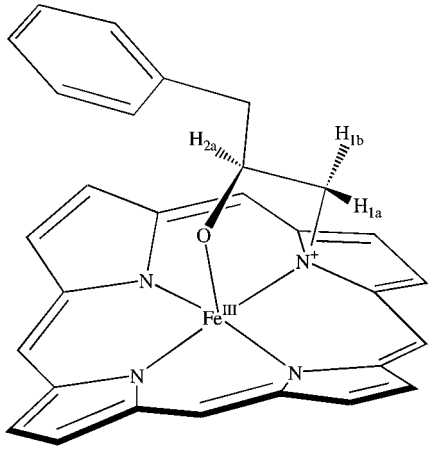

Figure 8. Structure of AB-CPO (structure **8**) calculated by MM2 energy minimization.

indicating close proximity to Fe. Those for H_{1a} and H_{1b} (C-1 position) are weak and overwhelmingly dipolar, and place these hydrogens above the nitrogen, N_a (Figure 6). These observations select structure **2** with R = CH_2Ph and R′ = H. The absence of solvent exchangeable protons in the electrospray mass spectra and the ^{1}H ENDOR further excludes the structures **3** and **4**.[36] Thus, we conclude that the alkene adds to the heme so as to place the 2-carbon closest to the iron, generating a "primary" N-alkylhemin that we now show to adopt structure **8**.

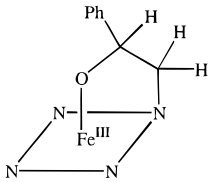

8

The absence of an ENDOR signal from strongly-coupled exchangeable proton(s) argues against the presence of an axial H_xO. The strong coupling to H_{2a} could not arise solely from spin polarization through the N_a−C1 linkage, and thus argues for the presence of the metallocycle **8**, formed by the Fe−O bond of the bound alkoxide. Nevertheless, the ENDOR measurements have not directly detected the axial alkoxide ligand, and thus the presence of the metallocycle, and in any case one wishes for greater structural detail. To both test and refine structure **8**, we have compared the ENDOR data with a MM2 energy minimization of this structure.[37] The lowest energy conformation of structure **8** is shown in Figure 8. In the absence of further information, we modeled the allylbenzene heme adduct by assuming that the oxoferryl group of compound **I** (Scheme 1) adds to the *re*face of the alkene.

Figure 9 expands the region of Figure 8 that contains the AB-heme metallocycle and includes nitrogen, N_a; it displays both the metrical parameters given by ENDOR and those taken from the MM2 refined structure **8**. In general, the parameters from the experiment and the refinement are in exceptionally good agreement. The higher quality agreement for H_{1a},

(35) (a) Mansuy, D.; Lange, M.; Chottard, J.-C.; Guerin, P.; Morliere, P.; Brault, D.; Rougee, M. *J. Chem. Soc., Chem. Commun.* **1977**, 648−649. (b) Mansuy, D.; Lange, M.; Chottard, J. C.; Bartoli, J. F.; Chevrier, B.; Weiss, R. *Angew. Chem., Int. Ed. Engl.* **1978**, *17*, 781−782. (c) Mansuy, D.; Battioni, J.-P.; Chottard, J.-C.; Ullrich, V. *J. Am. Chem. Soc.* **1979**, *101*, 3971−3973 and references therein. (d) Mansuy, D. *Pure Appl. Chem.* **1980**, *52*, 681−690. (e) Balch, A. L.; Chan, Y. W.; Olmstead, M. M.; Renner, M. W. *J. Org. Chem.* **1986**, *51*, 4651−4656. (f) Mansuy, D.; Battioni, J.-P.; Lavallee, D. K.; Fischer, J.; Weiss, R. *Inorg. Chem.* **1988**, *27*, 1052−1056.

(36) The formation of hemin dimers in the MS samples shows that the heme becomes separated from the apoprotein and is not sequestered from, and thereby prevented from exchanging with, the aqueous medium.

(37) An analogous approach of comparing results from ENDOR and molecular modeling has been used to study the structure of Rieske [2Fe−2S] cluster: Gurbiel, R. J.; Doan, P. E.; Gassner, G. T.; Macke, T. J.; Case, D. A.; Ohnishi, T.; Fee, J. A.; Ballou, D. P.; Hoffman, B. M. *Biochemistry* **1996**, *35*, 7834−7845.

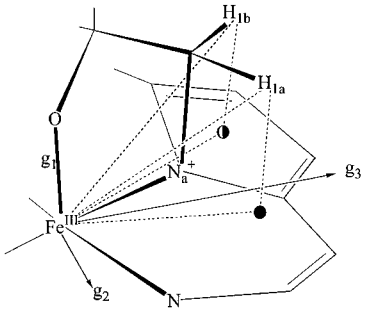

	ENDOR	MM2
(N_a^+-Fe^{III}-g_3)	15(5)°	-
(g_1-Fe^{III}-H_{1a})	56(5)°	55°
(g_1-Fe^{III}-H_{1b})	71(15)°	60°
(N_a^+-Fe^{III}-●)	22(8)°	28°
(N_a^+-Fe^{III}-◑)	21(15)°	5°
d(Fe^{III}-H_{1a})	3.1(05) A	3.2 A
d(Fe^{III}-H_{1b})	3.6(15) A	3.7 A

Figure 9. Comparison of structures determined by ENDOR and MM2. ● and ◑ are the projections of H_{1a} and H_{1b} onto the heme plane. The (g_1−Fe^{III}−H_1) MM2 angles are obtained by the assumption that the g_1 axis is identical to the Fe^{III}−O bond.

compared to H_{1b}, reflects the fact that ^2H ENDOR data for H_{1b} are available only at a few field positions, and thus the hyperfine tensor is not as well constrained. Overall, the MM2 calculation both confirms and extends the ENDOR analysis of the structure of the heme of AB-CPO. The agreement of the measured and calculated Fe−H_1 distances confirms that inactivation occurs by regioselective bonding of C-1 to the pyrrole nitrogen. The agreement between the ENDOR and MM2 structures, both distances and angles, coupled with the ENDOR evidence for a large coupling to H_{2a} and against an alternate proximal ligand such as water or hydroxide in our view is conclusive confirmation that the alkoxide oxygen ligates to the heme iron to give the metallocycle of structure **8** as visualized in Figure 8.[38]

Discussion

In the present work, we have investigated for the first time the *in situ* structure of an alkene-modified enzymatic heme. While the results have confirmed earlier conclusions regarding the occurrence of structure **2**, they provide a detailed view of the regiochemistry of alkene addition and indeed metrical parameters, as well as serving as a foundation for further studies of this and related systems. In particular, determination that **8** represents the heme structure of AB-CPO is an important prerequisite for understanding the catalytic mechanism of CPO, the mechanism of spontaneous heme dealkylation and restoration of catalytic activity in this system,[7] as well as the susceptibility of the enzyme to inactivation with different olefinic substrates.[3a] The ENDOR-based structural assignment may also serve as a basis for studies of the modified enzyme using other spectroscopic techniques.

The orientation of allylbenzene addition to the heme in CPO is consistent with results obtained with terminal alkenes in P450[4] and in model tetraarylhemins containing bulky *o*-aryl substituents.[5,6] In these sterically hindered hemins, "secondary" N-alkylated hemins[6c] are minor and unstable products of the reaction with terminal alkenes. Formation of secondary N-alkylhemins has not been demonstrated in any enzyme system to date, nor do disubstituted alkenes inactivate P450 or CPO. In tetraarylhemins where the aryl groups lack bulky *ortho* substituents, secondary N-alkylhemins may be formed as major products with terminal alkenes.[5c] Secondary *N*-alkylhemins may also be formed in model systems as adducts with disubstituted alkenes.[5d,6b,c] We have recently obtained evidence for steric control in the partitioning between *N*-alkylhemin formation and epoxidation during oxidation of terminal alkenes by CPO and have shown that with appropriate alkene substrates, N-alkylation is an order of magnitude more facile in CPO than previously reported in any other heme system.[3a] The alkylation of a specific pyrrole nitrogen indicated in this study, together with demonstrations of regioselective heme alkylation in P450,[4a] suggests that steric factors control the site of pyrrole alkylation in enzyme systems, as well as the orientation of alkene addition to the heme face. Based on the substrate selectivity and partition numbers,[3a] heme N-alkylation in CPO appears to be under greater steric control than in model systems,[5g] possibly as a result of heme occlusion by the protein structure.

The results obtained in this study may comment to a limited extent on the mechanism of CPO-catalyzed epoxidation. In P450, the formation of organometallic porphyrin species during alkene epoxidation was originally proposed to explain exchange of the vinylic protons of propene with the aqueous medium under oxidizing conditions,[9a] although an alternate explanation for this result has since been offered.[9b] We do not observe exchange of the vinylic protons of allylbenzene with water in heme-alkylated CPO and can thus exclude species with exchangeable protons as long-lived precursors to **8**. This rules out Fe,N bridged species such as **3** and **4**, as well as the carbene **5** and *σ*-vinylhemin **6**, as precursor species partitioning between epoxidation and heme N-alkylation. It does not, however, exclude other proposed intermediates such as the four-membered metallocycle **9**,[39] the cation **10**,[6b] or the radical **11**.[40]

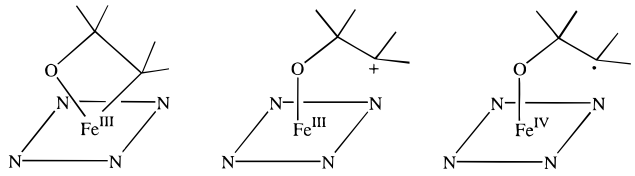

We find a radical species such as **11** an attractive proposal for an intermediate partitioning between heme N-alkylation and epoxidation, in part because of the specific susceptibility of iron porphyrins to the "suicide" reaction. To date, inactivation and pyrrole alkylation by alkenes has not been reported for Mn or Cr porphyrins during epoxidation, although these metalloporphyrins are well-studied epoxidation catalysts. It is tempting to propose that hemin N-alkylation is a specific consequence of the structure of the two-electron oxidized iron porphyrin species which reacts with alkenes. In iron porphyrins, this species is understood to be a Fe(IV) porphyrin cation radical,[41] while the corresponding two-electron oxidized species in Mn

(38) This study provides no direct evidence about bonding between the cysteine thiolate ligand and CPO heme in AB-CPO. To address this, we plan to carry out ^2H ENDOR studies of AB-CPO labeled with β-$^2H_2$-cysteine.

(39) (a) Collman, J. P.; Brauman, J. I.; Meunier, B.; Hayashi, T.; Kodadek, T.; Raybuck, S. A. *J. Am. Chem. Soc.* **1985**, *107*, 2000−2005. (b) Collman, J. P.; Kodadek, T.; Raybuck, S. A.; Brauman, J. I.; Papazian, L. M. *J. Am. Chem. Soc.* **1985**, *107*, 4343−4345. (c) Collman, J. P.; Kodadek, T.; Brauman, J. I. *J. Am. Chem. Soc.* **1986**, *108*, 2588−2594.

(40) Luke, B. T.; Collins, J. R.; Loew, G. H.; McLean, A. D. *J. Am. Chem. Soc.* **1990**, *112*, 8686−8691.

Scheme 2

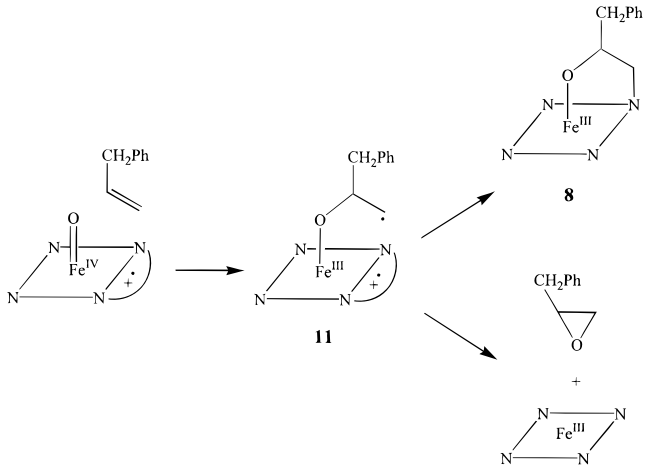

and Cr systems are metal(V) porphyrins.[42] Heme N-alkylation might be considered as bond formation between an alkene-derived free radical and the porphyrin ring radical in the oxidized hemin (Scheme 2). Direct evidence has recently been obtained for a radical species as an intermediate in epoxidation.[43] While the ENDOR and labeling studies described here would also be compatible with concerted epoxidation and heme N-alkylation mechanisms,[44] it is difficult to see how this mechanism accounts for the restriction of the pyrrole N-alkylation reaction to iron porphyrins.

Model metallocycles of type **2** return to the native hemin on standing, but do not revert at a sufficient rate to be an intermediate in the epoxidation pathway.[6b,c] We have obtained similar results in CPO, where the half-life for reversion of AB-CPO to the native enzyme is 5.8 h at 25 °C.[7] In model systems, but not enzymatic systems, the N-alkylated metallocycle is still an epoxidation catalyst, although it has reduced catalytic activity.[5f,6] Synthetic N-alkylhemins have been shown directly to be capable of forming the two-electron oxidized species which act as oxygen donors in epoxidation.[45] The inability of alkene-modified CPO to similarly form oxidized species and catalyze substrate oxidation[3a,7] might possibly be attributed to inaccessibility to oxidant of the second heme axial site in the intact enzyme. In contrast, five-coordinate model N-alkylhemins can function as oxygen donors on the remaining free heme face.

The ^{14}N and ^{15}N ENDOR of allylbenzene-inactivated CPO indicates that the pyrrole alkylation is highly regioselective. A single set of heme pyrrole signals (comprising three similar nitrogens and one greatly shifted nitrogen) is observed in the ENDOR samples, without detectable contributions from products in which a different pyrrole nitrogen has been alkylated. Although we cannot exclude the possibility that small amounts of alternate alkylation products are present in the intact enzyme, the ENDOR results show that pyrrole alkylation occurs largely at one site, consistent with results obtained in P450.[4a] Studies are now underway to determine the specific site of alkylation in the isolated N-alkylporphyrin, as well as the enantioselectivity at C-2 of heme adduct formation.

In summary, these first detailed spectroscopic and structural studies of an alkene-inactivated heme enzyme show that the heme of AB-CPO has structure **8** (Figure 8). It is hoped that these results may stimulate similar studies of alkene inactivation of P450 as the sister enzyme of CPO.

Acknowledgment. This work was supported by the National Institutes of Health (HL 13531 (B.M.H.) and GM 07768 (L.P.H.)). A.F.D. is the recipient of a Predoctoral Fellowship in Biological Sciences from the Howard Hughes Medical Institute. Positive ion electrospray mass spectra were recorded in the Mass Spectrometry Laboratory, School of Chemical Sciences, University of Illinois, using a Fisons VG Quattro quadrupole−hexapole−quadrupole mass spectrometer purchased in part with a grant from the Division of Research Resources, NIH (RR 07141).

JA963684C

(41) (a) Dolphin, D.; Forman, A.; Borg, D. C.; Fajer, J.; Felton, R. H. *Proc. Natl. Acad. Sci. U.S.A.* **1971**, *68*, 614−618. (b) Schulz, C. E.; Devaney, P. W.; Winkler, H.; Debrunner, P. G.; Doan, N.; Chiang, R.; Rutter, R.; Hager, L. P. *FEBS Lett.* **1979**, *103*, 102−105. (c) Roberts, J. E.; Hoffman, B. M.; Rutter, R.; Hager, L. P. *J. Biol. Chem.* **1981**, *256*, 2118−2121. (d) Roberts, J. E.; Hoffman, B. M.; Rutter, R.; Hager, L. P. *J. Am. Chem. Soc.* **1981**, *103*, 7654−7656.

(42) (a) Lee, W. A.; Bruice, T. C. *Inorg. Chem.* **1986**, *25*, 131−135. (b) Ostovic, D.; Bruice, T. C. *Acc. Chem. Res.* **1992**, *25*, 314−320.

(43) (a) Groves, J. T.; Watanabe, Y. *J. Am. Chem. Soc.* **1986**, *108*, 507−508. (b) Gross, Z.; Nimri, S. *J. Am. Chem. Soc.* **1995**, *117*, 8021−8022.

(44) In principle, the degree of stereochemical retention in the heme adduct could be determined by use of allylbenzene that has been stereospecifically labeled with one deuterium at C-1, and would comment on a stepwise *vs* concerted mechanism of adduct formation.

(45) Balch, A. L.; Cornman, C. R.; Latos-Grazynski, L.; Renner, M. W. *J. Am. Chem. Soc.* **1992**, *114*, 2230−2237.